Article

Graphene Quantums Dots Combined with Endonuclease Cleavage and Bidentate Chelation for Highly Sensitive Electrochemiluminescent DNA Biosensing

Jing Lou, Shanshan Liu, Wenwen Tu, and Zhihui Dai

Anal. Chem., **Just Accepted Manuscript** • DOI: 10.1021/ac5037318 • Publication Date (Web): 19 Dec 2014

Graphene Quantums Dots Combined with Endonuclease Cleavage and Bidentate Chelation for Highly Sensitive Electrochemiluminescent DNA Biosensing

Jing Lou, Shanshan Liu, Wenwen Tu,* and Zhihui Dai*

Jiangsu Collaborative Innovation Center of Biomedical Functional Materials and Jiangsu Key Laboratory of Biofunctional Materials, College of Chemistry and Materials Science, Nanjing Normal University, Nanjing, 210023, P. R. China

*Tel./Fax: +86-25-85891051. E-mail: daizhihuii@njnu.edu.cn, wwt@njnu.edu.cn.

ABSTRACT

A novel strategy for highly sensitive electrochemiluminescence (ECL) detection of DNA was proposed based on site-specific cleavage of BamHI endonuclease combining with the excellent ECL activity of graphene quantum dots (GQDs) and bidentate chelation of dithiocarbamate DNA (DTC-DNA) probe assembly. The difference between photoluminescence and ECL spectra peaks suggested the negligible defect existed on the GQDs surface for generating ECL signal. The formed DTC-DNA directly attached onto the gold surface by bidentate anchoring (S-Au-S bonds) which conferred a strong affinity between ligands and the Au surface, increasing the robustness of DNA immobilization on the gold surface. BamHI endonuclease site-specifically recognized and cleaved the duplex symmertrical sequence which made the double-strand DNA fragments and the GQDs break off from the electrode surface, inducing the decrease of ECL signal. Using HCV-1b cDNA (hepatitis C virus-1b genotype complementary DNA) as a model, a novel signal-off ECL DNA biosensor was developed based on the variation of ECL intensity before and after digesting the DNA hybrid. Electrochemical impedance spectroscopy confirmed the successful fabrication of the ECL DNA biosensor. This ECL biosensor for HCV-1b cDNA determination exhibited a linear range from 5 fM to 100 pM with a detection limit of 0.45 fM at a signal-to-noise ratio of 3, and showed satisfactory selectivity and good stability, which validated the feasibility of the designed strategy. The proposed strategy may be conveniently combined with other specific biological recognition events for expanding biosensing application, especially in clinical diagnoses.

INTRODUCTION

Rapid and sensitive detection of specific DNA with ultralow concentrations has attracted considerable interest due to its broad applications in infectious diseases, genetic therapy and early screening of diseases.[1] In recent years, numerous DNA detection systems have been proposed for the detection of DNA sequences by photoelectrochemical,[2] optical,[3,4] electrochemical[5] or electrochemiluminescence (ECL)[6,7] techniques. The effective immobilization of DNA probe have been considered as an essential factor to develop efficient DNA biosensor for its applications in clinical assay and diagnoses.[8] In order to enhance stability of the probe DNA immobilized on electrode surface, various immobilization strategies such as covalent coupling,[9,10] adsorption,[11] cross-linking[12] and copolymerization[13] have been explored. Among these methods, self-assembled monolayer of thiolated single-strand DNA (ssDNA) chemisorbed on the gold surface was the most widespread immobilization strategy.[14,15] However, the thiolated ssDNA was easily oxidized by the oxidizing agents present in solution.[16] Thus, a simple and effective strategy for DNA immobilization on gold electrode surface was urgent to establish. In this work, amine-modified oligonucleotides easily reacted with CS_2 to generate DNA with dithiocarbamate (DTC) ligands *in situ.*[17] The formed DTC-DNA directly attached onto the gold surface by bidentate anchoring (S-Au-S bonds) which conferred a stronger affinity between ligands and the Au surface than that of the thiolated ssDNA linked to the gold surface (Au-S bond), increasing the robustness of DNA immobilization on the gold surface. In addition, the restriction endonuclease was a well-studied class of DNA-binding proteins which played significant roles in life processes, such as DNA replication, recombination, repair, genotyping.[18-20] Its highly specific interactions with their DNA recognition sites provided exciting possibilities

for advanced development of novel analytical methods.[21] Through the endonuclease-stimulated regeneration of the analyte, the fluorescent aptasensors have been designed to detect adenosine triphosphate, vasopressin and cocaine.[22] Based on site-specific cleavage of BamHI endonuclease and enzymatic signal amplification, a electrochemical method to detect hepatitis C virus was developed.[23]

Electrochemiluminescence (ECL), which combined the chemiluminescence with electrochemistry techniques and exhibited its unique advantages, such as its simplified set-up, low background signal and high sensitivity.[24] As ECL luminophores, gold clusters, cadmium-containing quantum dots (QDs) and carbon dots have been extensively reported in recent years.[25-27] Graphene quantum dots (GQDs), as the new member of the nanocarbon family, compared with the gold cluster, cadmium-containing QDs and carbon dots, exhibited low costly, large specific surface area, unique electro-optical properties, low toxicity, robust chemical inertness and attractive biocompatibility.[28-32] Especially, GQDs have been used to construct a few ECL sensors, such as the ECL sensor for detection of Cd^{2+}[29] and Pb^{2+}[33] which became promising to substitute traditional QDs as ECL luminophores. Moreover, only one work referred to the ECL DNA biosensors based on GQDs up to now,[34] which was based on resonance energy transfer between GQDs and gold nanoparticles for DNA detection. However, its low sensitivity limited its application. This work designed a novel strategy for highly sensitive ECL detection of DNA based on site-specific cleavage of BamHI endonuclease combining with the excellent ECL activity of GQDs and bidentate chelation of dithiocarbamate DNA probe assembly. Obviously, its strategy was different from the previous report.[34] In addition, its anlytical performance was much better than the previous report.[34]

Herein, a novel strategy for highly sensitive electrochemiluminescence (ECL) detection of DNA was proposed based on site-specific cleavage of BamHI endonuclease combining with the excellent ECL activity of graphene quantum dots (GQDs) and bidentate chelation of dithiocarbamate DNA (DTC-DNA) probe assembly. Using HCV-1b cDNA (hepatitis C virus-1b genotype complementary DNA) as a model, the BamHI endonuclease site-specifically recognized and cleaved the duplex symmertrical sequence 5'-GGATCC-3'[35] which made the double-strand DNA (dsDNA) fragments and the GQDs break off from the electrode surface, leading to the decline of ECL intensity. Based on the variation of ECL intensity before and after digesting the DNA hybrid, a novel signal-off ECL DNA biosensor was developed (Scheme 1). Moreover, the probe DTC-DNA with dithiocarbamate ligands directly assembled on the gold surface by bidentate chelation enhanced the robustness of DNA immobilization, improving stability of this biosensor. This designed signal-off ECL DNA biosensor exhibited good analytical performance which provided an alternative method for highly sensitive determination of DNA.

EXPERIMENTAL SECTION

Materials and Reagents. Tris(hydroxymethyl) aminomethane (Tris) was purchased from Alfa Aesar Company. 3-mercapto-1-hexanol (MCH), N-hydroxysuccinimide (NHS, 98%) and N-(3-dimethylaminopropyl)-N′-ethylcarbodiimide (EDC) were purchased from Sigma-Aldrich Company. BamHI endonuclease was obtained from New England Biolabs Ltd (United Kingdom). Citric acid monohydrate (CA), carbon disulfide (CS_2) and ethylenediamine were obtained from Sinopharm Chemical Reagent Co, Ltd (Shanghai, China). Other chemicals were of analytical reagent grade. Tris-HCl buffer saline (0.05 mol L^{-1}, pH 7.4) containing 0.1 M $K_2S_2O_8$ and 0.1 M KCl was used as

test solution. The pH value of the Tris-HCl buffer saline was 7.4 except where otherwise indicated. The washing solution was 0.01 M Tris-HCl buffer saline. Ultrapure water obtained from a water purification system (≥18 MΩ·cm, MST-I-10, Shanghai Mosu Science Equipment Co, Ltd, China) was used in all measurements. The DNA strands were purchased from Sangon Biological Engineering Technology&Company Ltd. (Shanghai, China) and purified with high-performance-liquid chromatography. Their base sequences were listed as below.

Probe DNA: 5′-COOH-AACGTCGGATCCCGCGTCGCC-$(CH_2)_6$-NH_2-3′

Target DNA: 5′-GGCGACGCGGGATCCGACGTT -3′

M1: 5′-GGCGACGCGGG***T***TCCGACGTT -3′

M2: 5′-GGCG***T***CGCGGGATCCGACGTT -3′

M3: 5′-GGCGA***G***GCGGGATCC***C***ACGTT -3′

Apparatus. The ECL emission was detected with an MPI-A electrochemiluminescence analyzer (Xi′An Remax Electronic Science &Technology Co. Ltd., Xi′An, China). All experiments were carried out at room temperature using a conventional three-electrode system with a modified gold electrode (GE) (2 mm diameter) as working electrode, a platinum wire as the auxiliary electrode and an Ag/AgCl electrode as reference electrode. The emission window was placed in front of the photomultiplier tube, which was biased at 800 V. Ultraviolet-visible (UV-vis) absorption spectra were obtained on Cary 50 spectrophotometer (Varian, USA). Photoluminescence (PL) spectra were recorded on Cary Eclipse spectrometer (Varian, USA). Electrochemical impedance spectroscopy (EIS) was carried out with an Autolab potentiostat/galvanostat PGSTAT302N (Eco chemie, BV, The Netherlands) and cotrolled by Nova 1.10 soft-ware with a three-electrode system, in KCl solution (0.1 mol L^{-1}) containing a $K_3Fe(CN)_6/K_4Fe(CN)_6$ (5.0 mmol L^{-1}) (1:1) mixture as a

redox probe from 0.1 Hz-100KHz with a signal amplitude of 10 mV. Transmission electrochemical microscope (TEM) image was taken using a Hitachi H-7650 type transmission electron microscope at an accelerating voltage of 80 kV (Hitachi, Japan). Fourier transform infrared (FTIR) spectrum was acquired on Tensor 27 (Brucker, Germany) in the range of 400-4000cm^{-1} at room temperature.

Synthesis of GQDs and DTC-DNA. The GQDs were synthesized according to the previous report[36] with modification. Briefly, 2 g citric acid was put into a 5 mL beaker and heated to 200 ˚C by a heating mantle for 30 min, until the citric acid of white solid changed to an orange liquid. Then, a certain amount of 10 mg mL^{-1} NaOH solution was added into the orange liquid drop by drop, with continuously vigorous stirring, until the pH value of the solution was adjusted to 7 to obtain GQDs solution. The attained GQDs solution was stored at 4 ˚C in the refrigerator.

Dithiocarbamate (DTC)-DNA was prepared with amine-modified ssDNA according to the previous work.[17] Briefly, 100 μM CS_2 reacted with equimolar concentration of amine-modified ssDNA in 10 mM borate buffer saline (pH 9.0) for 1 h under stirring, and then DTC-DNA was obtained.

Fabrication of ECL DNA Biosensor. The gold electrode was polished carefully with 0.05um α-Al_2O_3 powders on chamois leathers and washed ultrasonically with water and ethanol, respectively. Then the electrode was electrochemically cleaned in 0.5 M H_2SO_4 solution with scanning from -0.3 and 1.6 V, followed by drying under nitrogen. DTC-DNA (4 μL, 1 μM) was dropped on the GE and kept overnight at 4 ˚C, followed by washing to remove non-grafted DNA. The amount of probe DNA on the electrode surface was excessive which should result in a saturated layer on the surface of the electrode. Thus the probe DNA fully covered electrode surface. DTC-DNA assembled on the GE via bidentate chelation (S-Au-S

bonds). Afterwards, the DTC-DNA modified GE was immersed into 1 mM MCH solution for 1 h to block the uncovered surface and reduce the nonspecific adsorption, and then rinsed. Subsequently, DTC-DNA/MCH modified GE was activated by immersion in the EDC-NHS mixture (5 mM EDC, 10 mM NHS in 10 mM Tris-HCl buffer saline, pH7.4) for 40 minutes. Then 4 μL ethylenediamine solution (4.0 wt %) was dropped on the electrode surface and dried under air to obtain DTC-DNA/MCH/ethylenediamine modified GE. Finally, 4 μL GQDs solution was dropped onto electrode. After rinsing with 0.01 M Tris-HCl buffer saline, the ECL DNA biosensor was obtained.

Measurement Procedure. 5 μL different concentrations of target DNA were applied to DTC-DNA/MCH/ethylenedianmine/GQDs modified GE and incubated at 37 ˚C for 2 h. The different electrodes were used for hybridization of target DNA from low concentration to high value. Subsequently, the modified GE was swilled thoroughly to remove unbounded target DNA. Then BamHI endonuclease cleavage was performed by incubating the dsDNA hybrid in Tris-HCl buffer saline containing BamHI endonuclease (20 U/μL), $MgCl_2$ (10 mM) and NaCl (100 mM) at 37 ˚C for 2 h. After cleavage, the DTC-DNA/MCH/ethylenedianmine/GQDs/target/BamHI modified GE was thoroughly washed and transferred into Tris-HCl buffer saline (0.05 M, pH 7.4) containing 0.1 M $K_2S_2O_8$ and 0.1 M KCl to record the ECL response of the biosensor between 0 and -2.0 V at 100 mV s^{-1}. The emission window was placed in front of the photomultiplier tube, which was biased at 800 V.

RESULTS AND DISCUSSION

Characterization. As shown in TEM image (Figure 1A), although some parts of the GQDs were shown to be in close touch, they were well dispersed in aqueous solution. The well dispersion of GQDs was beneficial for electron transfer between

GQDs and electrode, which was advantageous for construction of highly sensitive ECL biosensor. In addition, the size of the GQDs was estimated to be 20 nm (Figure 1A, inset). FTIR spectrum was used to characterize the carboxyl group on GQDs (Figure 1B). The C=O and O-H stretching vibrations of the carboxyl group were observed at 1729 and 3454 cm^{-1}, respectively. In addition, C-O and O-H deformation peak at 1404 and 1220 cm^{-1}, respectively also appeared. These results suggested that the surface of GQDs existed carboxyl group.

UV-vis absorption and PL spectra were used to further confirm the formation of GQDs (Figure 2). The UV-vis absorption of GQDs showed a well-defined absorption band at 348 nm while that of citric acid exhibited no obvious absorption from 305 to 800 nm (Figure 2A), indicating the formation of GQDs prepared by directly pyrolyzing citric acid.[36] At the concentration of 1.4 mg mL^{-1}, the solution of GQDs was homogeneous and was very stable, even for a storage period of several months (Figure 2A, inset). The solution of GQDs presented blue under UV light irradiation while it showed colorless and transparent under visible light irradiation. The deeper color of GQDs under UV light irradiation suggested the formation of GQDs. The PL spectra of GQDs solution exhibited the maximum emission wavelength at 465 nm with the maximum excitation wavelength at 385 nm (Figure 2B), which also verified the successful preparation of GQDs.[36]

EIS effectively investigated the stepwise assembly process of the DNA biosensor. As shown in Figure 3A, the bare Au electrode exhibited a lowest electron-transfer resistance (R_{et}) towards the redox couple (curve a). When the DTC-DNA was coated onto the Au electrode, R_{et} increased significantly (curve b), which was attributed to that the negatively charged phosphate backbone of DTC-DNA repelled the transfer of the negatively charged probe ($Fe(CN)_6^{3-/4-}$). After the DTC-DNA modified electrode

was immersed into 1 mM MCH solution, R_{et} further increased owing to its poor conductivity (curve c). However, R_{et} decreased dramatically after ethylenediamine was immobilized on the electrode via EDC/NHS activation (curve d), which might be attributed to that the ethylenediamine with positively charge attracted the negatively charged probe ($Fe(CN)_6^{3-/4-}$). Subsequently, R_{et} increased a little when the GQDs covalently bonded to the ethylenediamine through the interaction between amine and carboxyl groups (curve e), which indicated that the GQDs were successfully bond to the ethylenediamine. R_{et} further increased after hybridizing with target DNA (curve f), implying an efficient DNA hybridization occurred on the modified electrode surface. In order to demonstrate the efficient hybridization, probe DNA hybridized with a series of concentrations of target DNA. As shown in Figure 3B, R_{et} increased step by step after hybridizing with 0.5 pM (curve a), 1 pM (curve b), 5 pM (curve c) and 10 pM (curve d) target DNA, respectively, indicating the efficient hybridization. After the DTC-DNA/MCH/ethylenedianmine/GQDs/target modified electrode was treated with BamHI, R_{et} decreased (curve g). The decreased R_{et} could be attributed to the following reason. BamHI cleaved the dsDNA, and then the dsDNA fragments and the GQDs were broken off from the electrode surface, which weakened the steric hindrance and accelerated the electron transfer between the redox probe and electrode surface. These changes of electron transfer resistance verified the successful fabrication of the ECL DNA biosensing interface.

ECL Behaviors. As shown in Figure S-1A of the Supporting Information, upon successive scans for 8 cycles, the DTC-DNA/ethylenediamine/GQDs/target (0.5 pM)/BamHI modified GE showed stability cyclic voltammogram (CV) peaks, apart from the reduction peak of $S_2O_8^{2-}$ at about -0.85 V,[29] the CV curve of DTC-DNA/ethylenediamine/GQDs/target/BamHI modified GE showed a weak

reduction peak at about -1.33 V (Figure 4A). This weak peak might be assigned to the reduction peak of GQDs.[29] The control experiments (Figure S-2 of the Supporting Information) were performed to further confirm the weak peak was attributed to GQDs. The bare gold electrode showed a reduction peak of $S_2O_8^{2-}$ (curve a), after layer by layer assembly, the DTC-DNA (curve b), DTC-DNA/MCH (curve c) and DTC-DNA/MCH/ethylenediamine (curve d) modified GEs also showed a reduction peak of $S_2O_8^{2-}$. However, when the GQDs covalently bonded to the ethylenediamine through the interaction between amine and carboxyl groups, apart from the reduction peak of $S_2O_8^{2-}$, the DTC-DNA/MCH/ethylenediamine/GQDs modified GE showed another weak peak (curve e) which might be attribute to the reduction of GQDs. As shown in Figure 4B, the ECL spectra of GQDs obtained from optical filter with a series of wavelength showed the emission peak at 474 nm, while the PL emission spectrum of GQDs exhibited the peak at 464 nm (excited at 385 nm). This 10 nm difference of spectra peak suggested that the GQDs surface existed negligible defect for producing ECL signal.[29,37]

As shown in Figure 4C, the reduction of GQDs started at about -0.85 V with an intense ECL emission at -1.97 V. GQDs modified GE was that 4 μL GQDs dropped on the gold electrode and then dried under the air. Subsequently, GQDs modified GE was transferred into Tris-HCl buffer saline (0.05 M, pH 7.4) containing 0.1 M $K_2S_2O_8$ and 0.1 M KCl to record the ECL response between 0 and -2.0 V at 100 mV s^{-1}. The emission window was placed in front of the photomultiplier tube, which was biased at 800 V. In Figure 7B, upon successive scans for 7 cycles, the ECL intensity tended to level off with relative standard deviation of 1.9 %, which suggested that the DNA biosensor possessed good stability. These results validated that desorption of the thiol molecules and other derivatives have little effect on the ECL DNA biosensor. Herein,

it need be pointed out that the potential range scanned from 0 to -2 V has been extensively reported[24,38,39] and some papers have reported that the potential was more negative than -0.8 V when the thiol molecules were applied to fabricating ECL biosensors.[40-42] Moreover, no obvious change of the ECL intensity was observed after scanned by consecutive cyclic voltammograms for 8 cycles (Figure S-1B of the Supporting Information), indicating good stability of GQDs. To be honest, -2 V is not a good potential for ECL. Under this potential, many side reactions typically including hydrogen evolution and desorption of materials would lower the stability of the fabricated biosensors. We will focus on finding suitable materials with redox activity before -1 V or +1 V in our future work.

The bare GE was transferred into Tris-HCl buffer saline (0.05 M, pH 7.4) (Figure S-3A of the Supporting Information) and Tris-HCl buffer saline (0.05 M, pH 7.4) containing 0.1 M KCl (Figure S-3B of the Supporting Information) to record the ECL response between 0 and -2.0 V at 100 mV s^{-1}. The emission window was placed in front of the photomultiplier tube, which was biased at 800 V. ECL signal was not observed in Figure S-3A and Figure S-3B. However, when the bare GE was transferred into the Tris-HCl buffer saline (0.05 M, pH 7.4) containing 0.1 M $K_2S_2O_8$, an obvious ECL response appeared (Figure S-3C of the Supporting Information). The results indicated that the origination of ECL response of the bare GE might be from the $K_2S_2O_8$. The similar phenomenon was reported in the previous researches.[43,44] The $K_2S_2O_8$ was the coreactant of the GQDs, which was the essential of this system. Nevertheless, the ECL intensity of the $K_2S_2O_8$ was negligible compared with the ECL intensity of GQDs. After stepwise assembly of the electrode, the ECL intensity (Figure 4D, curve b) is about 5.6-fold of that observed from bare GE (Figure 4D, curve a) owing to its immobilization of GQDs on the GE. Excitingly, an obvious

decrease of ECL intensity occurred after the electrode was treated with BamHI (Figure 4D, curve c). This phenomenon was because BamHI endonuclease could recognize the duplex symmertrical sequence 5'-GGATCC-3' and catalyze the dsDNA cleavage[35], which made the dsDNA fragments and the GQDs break off from the electrode surface. The abscission of GQDs greatly declined the ECL intensity.

The probable ECL mechanism of the GQDs was proposed as follows.[29] For one thing, the GQDs immobilized on the electrode were reduced to $GQDs^{\bullet-}$ by charge injection, while the strongly oxidative $SO_4^{\bullet-}$ radicals were generated by electrochemical reduction of the coreactant $S_2O_8^{2-}$. For another, $GQDs^{\bullet-}$ could react with $SO_4^{\bullet-}$ to emit light in the aqueous solution. The possible ECL mechanisms were described with the following equations:

$$GQDs + ne^- \rightarrow nGQDs^{\bullet-} \quad (1)$$

$$S_2O_8^{2-} + e^- \rightarrow S_2O_8^{\bullet 2-} \quad (2)$$

$$S_2O_8^{\bullet 2-} \rightarrow SO_4^{2-} + SO_4^{\bullet-} \quad (3)$$

$$GQDs^{\bullet-} + SO_4^{\bullet-} \rightarrow GQDs^* + SO_4^{2-} \quad (4)$$

$$GQDs^* \rightarrow GQDs + h\nu \quad (5)$$

Optimization of Detection Conditions. The concentration of the probe DNA was a significant factor relevant to the ECL response. As the concentration of the probe DNA was in the range of 0.1 to 1 μM, the quantity of the GQDs attached onto the GE depended on the quantity of probe DNA. Therefore, the ECL intensity enhanced with the concentration of probe DNA increasing from 0.1 to 1 μM (Figure 5A). It arrived at a maximum at 1 μM. When the concentration of probe DNA was over 1 μM, the ECL response decreased. Excessive probe DNA immobilized on electrode increased the steric hindrance and hindered the electron transfer between GQDs and GE surface,

leading to the sharply decline of ECL intensity. Therefore, 1 μM was selected as the optimal concentration for ECL DNA biosensing.

The concentration of the GQDs was an important parameter for producing ECL signal. As shown in Figure 5B, with increasing the concentration of GQDs from 0.07 to 1.4 mg mL^{-1}, the intensity of photocurrent increased dramatically, and then tended to level off with only a slight decline from 1.4 to 3.5 mg mL^{-1}, indicating the equilibrium of GQDs concentration for generating ECL signal. As an ECL signal source, the concentration of 1.4 mg mL^{-1} was sufficient for ECL measurement in this system. As a result, 1.4 mg mL^{-1} was chosen as the optimal concentration.

ECL DNA Biosensing. Under the optimal conditions, the ECL responses to different concentrations of target DNA were investigated. Figure 6 displayed the ECL intensity of the DNA biosensor without (a) and with (b-j) of target DNA with different concentrations. In the presence of target DNA, the ECL intensity was lower than that in the absence of target DNA. The ECL intensity exhibited a linear decrease with increasing target DNA concentrations from 5 fM to 100 pM (Figure 6, inset). When the target DNA concentration was more than 100 pM, it would deviate the linear calibration curve. The calibration plot was constructed by plotting ECL intensity (I) against lg$C$ (C was different concentration of target DNA). The linear equation was I = 7300-1015lg(C_{target}) (6). The sensitivity was 32324 (ECL intensity cm^{-2}) which was much higher than 2547 (ECL intensity cm^{-2}) obtained by an ultrasensitive ECL DNA biosensor based on luminol functionalized gold nanoparticles.[1] The correlation coefficient was 0.9978, and the detection limit was estimated to be 0.45 fM at a signal-to-noise ratio of 3. The linear range was much wider or the detection limit was lower than some previously reported work (Table

1). [2-5,7,34,45] Therefore, this signal-off ECL DNA biosensor exhibited wide linear response range and high sensitivity in the determination of DNA.

Selectivity and Reproducibility of the ECL DNA Biosensor. To assess the selectivity of the proposed ECL detection method, the ECL responses of the designed biosensor to three mismatched target DNA with the same concentration (M1: with one mismatched base (T) is within the recognition sequence; M2: with one mismatched base (T) is not within the recognition sequence; M3: with two mismatched bases (G and C) are not within the recognition sequence) were investigated under the same experimental conditions (Figure 7A). In the presence of target DNA (column b) and M1 (column c), the ECL response decreased 43% and 16%, respectively, compared with that in the blank solution (column a), indicating a satisfactory selectivity of the as-prepared DNA biosensor. In addition, the decline of ECL response to target DNA (column b) was more obvious than that to M2 (column d) and M3 (column e). This level of mismatch discrimination ability was better than that of other previously reported endonuclease cleavage-based DNA biosensor.[46] Upon successive scans for 7 cycles (Figure 7B), the ECL intensity tended to level off with relative standard deviation of 1.9 %, which suggested that the DNA biosensor possessed good stability. These results validated the feasibility of the proposed strategy.

CONCLUSION

Using GQDs as a label and ECL signal source, combing with site-specific recognition of BamHI endonuclease and bidentate chelation of dithiocarbamate ligands for DNA probe assembly, a universal ECL biosensing platform was proposed. The solution of GQDs was homogeneous and was stable, exhibiting blue under UV light irradiation. This difference between PL and ECL spectra peaks suggested that the GQDs surface existed negligible defect for producing ECL signal. The probe DTC-DNA with

dithiocarbamate ligands directly assembled on the gold surface by bidentate chelation (S-Au-S bonds) enhanced the robustness of DNA immobilization, improving stability of this biosensor. BamHI endonuclease recognized the duplex symmertrical sequence and catalyzed the dsDNA cleavage which made the dsDNA fragments and the GQDs break off from the electrode surface, leading to the obvious decline of ECL intensity. Using HCV-1b cDNA as a model and combining with endonuclease cleavage and bidentate chelation, a novel ECL DNA biosensor was designed based on the variation of ECL intensity before and after digesting the DNA hybrid. This signal-off ECL DNA biosensor displayed good analytical performance, such as wide linear response range, high sensitivity, satisfactory selectivity and good stability. This designed strategy provided an alternative method for highly sensitive detection of DNA. Since different probes could specifically bind to different targets, this platform could be conveniently combined with other specific biological recognition events for extensive biosensing application.

ACKNOWLEDGEMENTS

This work was supported by the National Natural Science Foundation of China for the project (21475062, 21175069 and 21205061), Natural Science Foundation of Jiangsu (BK2012448), Research Fund for the Doctoral Program of Higher Education of China (20113207110005 and 20123207120007) and Foundation of the Jiangsu Education Committee (11KJA150003 and 12KJB150016). We appreciate the financial support from the Priority Academic Program Development of Jiangsu Higher Education Institutions.

ASSOCIATED CONTENT

Supporting Information Available

Additional information as noted in text. This information is available free of charge via the Internet at http://pubs.acs.org/.

AUTHOR INFORMATION

Corresponding Authors

* Tel./Fax: +86-25-85891051. E-mail: daizhihuii@njnu.edu.cn, wwt@njnu.edu.cn.

Notes

The authors declare no competing financial interest.

REFERENCES

(1) Chai, Y.; Tian, D.; Wang, W.; Cui, H. *Chem. Commun.* **2010**, *46*, 7560-7562.

(2) Yin, H. S.; Sun, B.; Zhou, Y. L.; Wang, M.; Xu, Z. N.; Fu, Z. L.; Ai, S. Y. *Biosens. Bioelectron.* **2014**, *51*, 103-108.

(3) Hu, R.; Liu, T.; Zhang, X. B.; Huan, S. Y.; Wu, C.; Fu, T.; Tan, W. *Anal. Chem.* **2014**, *86*, 5009-5016.

(4) Luo, M.; Chen, X.; Zhou, G. H.; Xiang, X.; Chen, L.; Ji, X. H.; He, Z. K. *Chem. Commun.* **2012**, *48*, 1126-1128.

(5) Liu, S. F.; Lin, Y.; Wang, L.; Liu, T.; Cheng, C. B.; Wei, W. J.; Tang, B. *Anal. Chem.* **2014**, *86*, 4008-4015.

(6) Shan, Y.; Xu, J. J.; Chen, H. Y. *Chem. Commun.* **2009**, 905-907.

(7) Li, F.; Yu, Y. Q.; Li, Q.; Zhou, M.; Cui, H. *Anal. Chem.* **2014**, *86*, 1608-1613.

(8) Sassolas, A.; Blum, L. J.; Leca-Bouvier, B. D. *Biotechnol. Adv.* **2012**, *30*, 489-511.

(9) Nie, G. M.; Bai, Z. M.; Yu, W. Y.; Chen, J. *Biomacromolecules* **2013**, *14*, 834-840.

(10) Wu, M. S.; Yuan, D. J.; Xu, J. J.; Chen, H. Y. *Anal. Chem.* **2013**, *85*, 11960-11965.

(11) Kaufmann, R.; Averbukh, I.; Naaman, R.; Daube, S. S. *Langmuir* **2008**, *24*, 927-931.

(12) Arrabito, G.; Reisewitz, S.; Dehmelt, L.; Bastiaens, P. I.; Pignataro, B.; Schroeder, H.; Niemeyer, C. M. *Small* **2013**, *9*, 4243-4249.

(13) Krpetic, Z.; Singh, I.; Su, W.; Guerrini, L.; Faulds, K.; Burley, G. A.; Graham, D. *J. Am. Chem. Soc.* **2012**, *134*, 8356-8359.

(14) Lou, X. H.; Zhao, T.; Liu, R.; Ma, J.; Xiao, Y. *Anal. Chem.* **2013**, *85*, 7574-7580.

(15) Hun, X.; Sun, W.; Zhu, H.; Du, F.; Liu, F.; Xu, Y.; He, Y. *Chem. Commun.* **2013**, *49*, 9603-9605.

(16) Schoenfisch, M. H.; Pemberton, J. E. *J. Am. Chem. Soc.* **1998**, *120*, 4502-4513.

(17) Sharma, J.; Chhabra, R.; Yan, H.; Liu, Y. *Chem. Commun.* **2008**, 2140-2142.

(18) Huang, Y.; Zhao, S. L.; Shi, M.; Chen, J.; Chen, Z. F.; Liang, H. *Anal. Chem.* **2011**, *83*, 8913-8918.

(19) Lee, J.; Kim, Y. K.; Min, D. H. *Anal. Chem.* **2011**, *83*, 8906-8912.

(20) Liu, S. N.; Hu, Y. J.; Jin, J.; Zhang, H.; Cai, C. X. *Chem. Commun.* **2009**, 1635-1637.

(21) Gerasimova, Y. V.; Kolpashchikov, D. M. *Chem. Soc. Rev.* **2014**.

(22) Lu, C. H.; Wang, F.; Willner, I. *Chemical Science* **2012**, *3*, 2616-2622.

(23) Tang, D. P.; Tang, J.; Su, B. L.; Li, Q. F.; Chen, G. N. *Chem. Commun.* **2011**, *47*, 9477-9479.

(24) Wu, L.; Wang, J.; Ren, J.; Li, W.; Qu, X. *Chem. Commun.* **2013**, *49*, 5675-5677.

(25) Li, L. L.; Liu, H. Y.; Shen, Y. Y.; Zhang, J. R.; Zhu, J. J. *Anal. Chem.* **2011**, *83*, 661-665.

(26) Han, E.; Ding, L.; Lian, H.; Ju, H. X. *Chem. Commun.* **2010**, *46*, 5446-5448.

(27) Zhang, P. J.; Xue, Z. J.; Luo, D.; Yu, W.; Guo, Z. H.; Wang, T. *Anal. Chem.* **2014**, *86*, 5620-5623.

(28) Yang, H. M.; Liu, W. Y.; Ma, C.; Zhang, Y.; Wang, X.; Yu, J. H.; Song, X. R. *Electrochim. Acta* **2014**, *123*, 470-476.

(29) Li, L. L.; Ji, J.; Fei, R.; Wang, C. Z.; Lu, Q.; Zhang, J. R.; Jiang, L. P.; Zhu, J. J. *Adv. Funct. Mater.* **2012**, *22*, 2971-2979.

(30) Li, Y.; Hu, Y.; Zhao, Y.; Shi, G. Q.; Deng, L. E.; Hou, Y. B.; Qu, L. T. *Adv. Mater.* **2011**, *23*, 776-780.

(31) Peng, J.; Gao, W.; Gupta, B. K.; Liu, Z.; Romero-Aburto, R.; Ge, L.; Song, L.; Alemany, L. B.; Zhan, X.; Gao, G.; Vithayathil, S. A.; Kaipparettu, B. A.; Marti, A. A.; Hayashi, T.; Zhu, J. J.; Ajayan, P. M. *Nano Lett.* **2012**, *12*, 844-849.

(32) Wang, Y.; Zhang, L.; Liang, R. P.; Bai, J. M.; Qiu, J. D. *Anal. Chem.* **2013**, *85*, 9148-9155.

(33) Dong, Y. Q.; Tian, W. R.; Ren, S. Y.; Dai, R. P.; Chi, Y. W.; Chen, G. N. *Acs Appl. Mater. Interfaces* **2014**, *6*, 1646-1651.

(34) Lu, Q.; Wei, W.;Zhou, Z.; Zhou, Z.; Zhang, Y.; Liu, S. *Analyst* **2014**, *139*, 2404-2410.

(35) Biggins, J. B.; Prudent, J. R.; Marshall, D. J.; Ruppen, M.; Thorson, J. S. *Proc. Natl. Acad. Sci. U.S.A.* **2000**, *97*, 13537-13542.

(36) Dong, Y. Q.; Shao, J. W.; Chen, C. Q.; Li, H.; Wang, R. X.; Chi, Y. W.; Lin, X. M.; Chen, G. N. *Carbon* **2012**, *50*, 4738-4743.

(37)Ji, J.; He, L.; Shen, Y. Y.; Hu, P. P.; Li, X. H.; Jiang, L. P.; Zhang, J. R.; Li, L. L.; Zhu, J. J. *Anal. Chem.* **2014**, *86*, 3284-3290.

(38) Zhang, J. J.; Wang, W. T.; Chen, S. H.; Ruo, Y.; Zhong, X.; Wu, X. P. *Biosens. Bioelectron.* **2014**, *57*, 71-76.

(39) Wu, L.; Wang, J. S.; Yin, M. L.; Ren, J. S.; Miyoshi, D.; Sugimoto, N.; Qu, X. G. *Small* **2014**, *10*, 330-336.

(40) Zhang, H.; Li, M.; Fan, M.; Gu, J.; Wu, P.; Cai, C. *Chem. Commun.* **2014**, *50*, 2932-2934.

(41) Zhang, H. R.; Wu, M. S.; Xu, J. J.; Chen, H. Y. *Anal. Chem.* **2014**, *86*, 3834-3840.

(42) Divsar, F.; Ju, H. X. *Chem. Commun.* **2011**, *47*, 9879-9881.

(43) Li, L. L.; Liu, K. P.; Yang, G. H.; Wang, C. M.; Zhang, J. R.; Zhu, J. J. *Adv. Funct. Mater.* **2011**, *21*, 869-878.

(44) Huang, H. P.; Zhu, J. J. *Biosens. Bioelectron.* **2009**, *25*, 927-930.

(45) Liu, P.; Yang, X. H.; Sun, S.; Wang, Q.; Wang, K. M.; Huang, J.; Liu, J. B.; He, L. L. *Anal. Chem.* **2013**, *85*, 7689-7695.

(46) Shen, Z. L.; Nakayama, S.; Semancik, S.; Sintim, H. O. *Chem. Commun.* **2012**, *48*, 7580-7582.

Table 1. The performance comparison of the proposed strategy with the previous reported researches.

Method	Detection limit (M)	Linear range (M)	materials	Refs.
Electrochemiluminescence	1.3×10^{-8}	2.5×10^{-8}-4×10^{-7}	graphene quantum dots	34
Fluorescence	2×10^{-11}	5×10^{-11}-1×10^{-10}	perylene diimide	3
Electrochemiluminescence	4×10^{-11}	1×10^{-10}-1×10^{-7}	$Ru(bpy)_3^{2+}$	7
Colorimetry	5×10^{-11}	5×10^{-11}-6×10^{-9}	gold nanoparticles	45
Electrochemistry	1×10^{-13}	1×10^{-13}-1×10^{-10}	ferrocene	5
Chemiluminescence	3.4×10^{-12}	1×10^{-10}-3×10^{-9}	luminol	4
Photoelectrochemistry	3.5×10^{-14}	1×10^{-13}-5×10^{-9}	Bi_2S_3 nanorods	2
Electrochemiluminescence	4.5×10^{-16}	5×10^{-15}-1×10^{-10}	graphene quantum dots	This work

FIGURE CAPTION

Scheme 1. Schematic illustration of the ECL biosensor based on GQDs combining with endonuclease cleavage and bidentate chelation.

Figure 1. (A) TEM image of GQDs. Inset: the size distribution of GQDs. (B) FTIR spectrum of GQDs.

Figure 2. (A) UV-Vis absorption spectra of CA and the GQDs, inset: photographs of the GQDs solution taken under visible light (left) and UV light (365 nm, right) irradiation. (B) PL spectra of the GQDs.

Figure 3. (A) EIS spectra of (a) bare GE, (b) DTC-DNA, (c) DTC-DNA/MCH, (d) DTC-DNA/MCH/ethylenediamine, (e) DTC-DNA/MCH/ethylenedianmine/GQDs, (f) DTC-DNA/MCH/ethylenedianmine/GQDs/target (0.5 pM) and (g) DTC-DNA/ MCH/ethylenedianmine/GQDs/target/BamHI modified GEs. Inset: expanded view of EIS spectra of (a), (d), (e), (f), (g). (B) EIS spectra of the proposed DNA biosensor to different concentrations of target DNA (0.5 pM (a), 1 pM (b), 5 pM (c) and 10 pM (d)).

Figure 4. (A) The CV curve of the DTC-DNA/ethylenediamine/GQDs/target(0.5 pM)/BamHI modified GE, (B) PL emission (λ_{ex} =385 nm) and ECL spectra of GQDs, (C) ECL response of GQDs modified GE during a continuous potential scan between 0 and -2.0 V, and (D) ECL responses of (a) bare GE, (b) DTC-DNA/MCH/ethylenediamine/GQDs/target(0.5 pM) and (c) DTC-DNA/MCH/ethylenediamine/GQDs/target(0.5 pM)/BamHI modified GEs in 0.05 M Tris-HCl buffer saline containing 0.1 M $K_2S_2O_8$ and 0.1 M KCl.

Figure 5. Effects of (A) probe DNA and (B) GQDs concentrations on the ECL response of the DNA biosensor in 0.05 M Tris-HCl buffer saline containing 0.1 M $K_2S_2O_8$ and 0.1 M KCl. The concentration of target was 0.5 pM.

Figure 6. ECL responses of the proposed DNA biosensor to different concentrations of target DNA (0, 5 fM, 10 fM, 50 fM, 0.1 pM, 0.5 pM, 1 pM, 5 pM, 10 pM, 100 pM, 200 pM and 500 pM from top to bottom) in 0.05 M Tris-HCl buffer saline containing 0.1 M $K_2S_2O_8$ and 0.1 M KCl between 0 and -2.0 V at 100 mV s^{-1}. The emission window was placed in front of the photomultiplier tube, which was biased at 800 V. Inset: linear calibration curve between the ECL intensity and the logarithm of the target DNA concentrations.

Figure 7. (A) ECL responses of the proposed DNA biosensor without (a) and with (b) 1 pM target DNA, (c) 1 pM M1, (d) 1 pM M2 and (e) 1 pM M3 in 0.05 M Tris-HCl buffer saline containing 0.1 M $K_2S_2O_8$ and 0.1 M KCl between 0 and -2.0 V at 100 mV s^{-1}. The emission window was placed in front of the photomultiplier tube, which was biased at 800 V. (B) ECL response of the DNA biosensor with 0.5 pM target DNA under continuous cyclic potential scan between 0 and -2.0 V for 7 cycles at 100 mV s^{-1}. The emission window was placed in front of the photomultiplier tube, which was biased at 800 V.

Scheme 1.

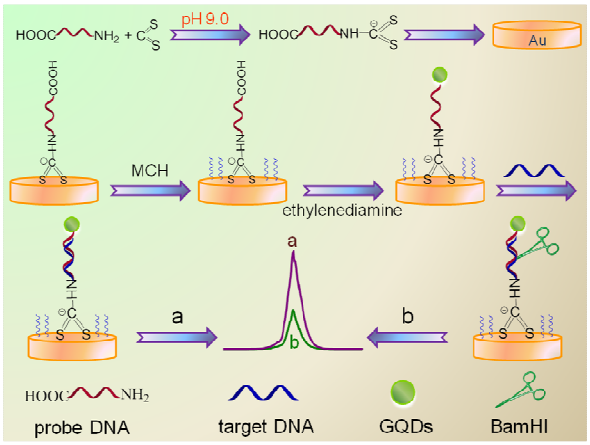

Figure 1.

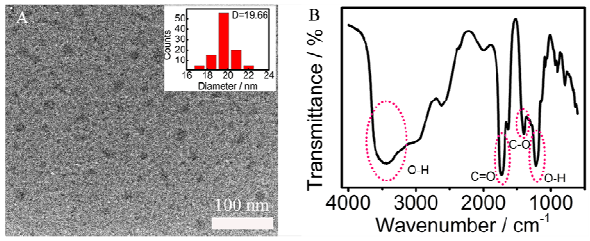

Figure 2.

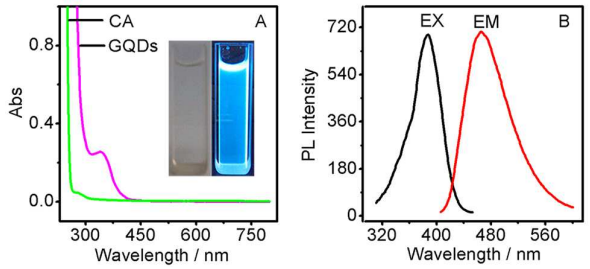

Figure 3.

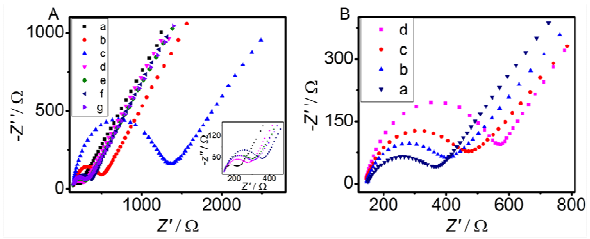

Figure 4.

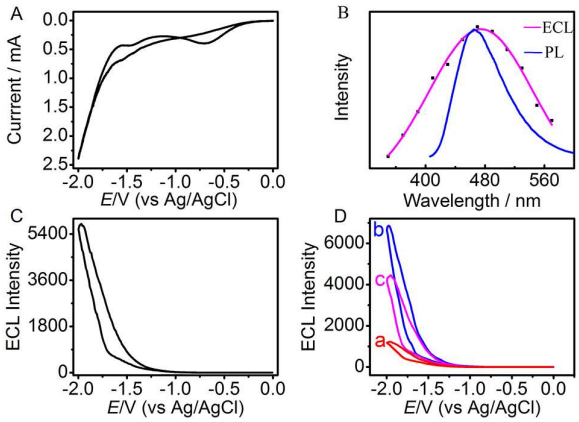

Figure 5.

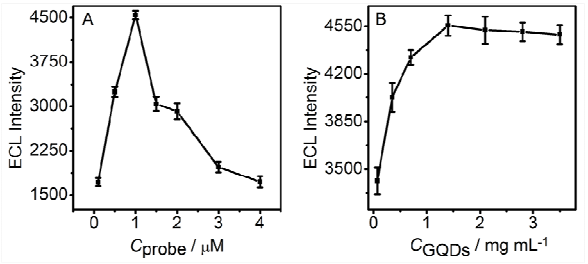

Figure 6.

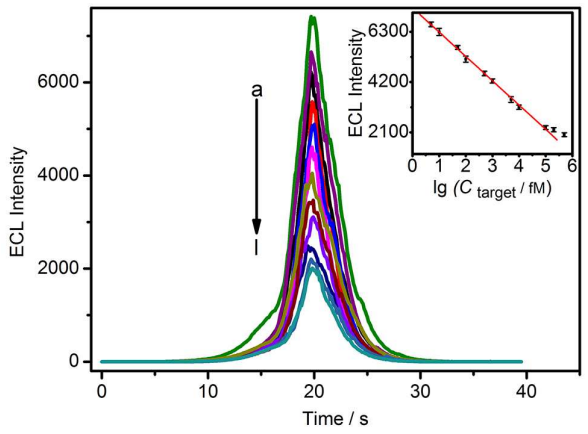

Figure 7.

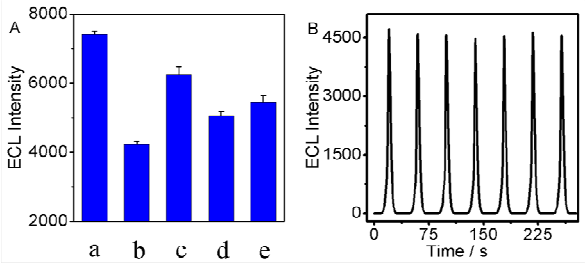

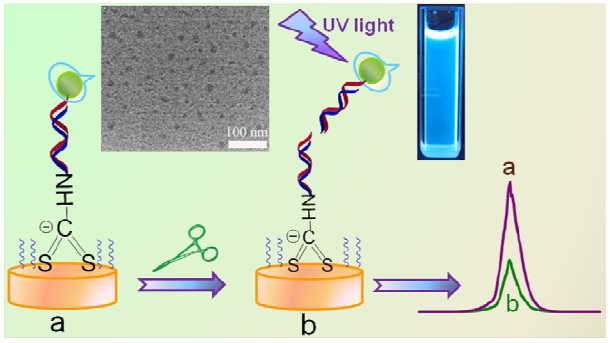

for TOC only